



Enriched fluoride sorption using alumina/chitosan composite

Natrayasamy Viswanathan^a, S. Meenakshi^{b,*}

^a Department of Chemistry, Anna University Tiruchirappalli – Dindigul Campus, Dindigul 624 622, Tamil Nadu, India

^b Department of Chemistry, Gandhigram Rural University, Gandhigram 624 302, Tamil Nadu, India

ARTICLE INFO

Article history:

Received 15 August 2009

Received in revised form 11 January 2010

Accepted 12 January 2010

Available online 18 January 2010

Keywords:

Alumina

Chitosan

Composite

Fluoride

Sorption

ABSTRACT

Alumina possesses an appreciable defluoridation capacity (DC) of 1566 mg F⁻/kg. In order to improve its DC, it is aimed to prepare alumina polymeric composites using the chitosan. Alumina/chitosan (AICs) composite was prepared by incorporating alumina particles in the chitosan polymeric matrix, which can be made into any desired form viz., beads, candles and membranes. AICs composite displayed a maximum DC of 3809 mg F⁻/kg than the alumina and chitosan (52 mg F⁻/kg). The fluoride removal studies were carried out in batch mode to optimize the equilibrium parameters viz., contact time, pH, co-anions and temperature. The equilibrium data was fitted with Freundlich and Langmuir isotherms to find the best fit for the sorption process. The calculated values of thermodynamic parameters indicate the nature of sorption. The surface characterisation of the sorbent was performed by FTIR, AFM and SEM with EDAX analysis. A possible mechanism of fluoride sorption by AICs composite has been proposed. Suitability of AICs composite at field conditions was tested with a field sample taken from a nearby fluoride-endemic village. This work provides a potential platform for the development of defluoridation technology.

© 2010 Elsevier B.V. All rights reserved.

1. Introduction

Fluorosis is an endemic public health problem prevails in 22 nations around the globe. The presence of fluoride content in potable water above the tolerance limit leads to fluorosis. Hence it is an important task to supply water with safe fluoride levels. Many efforts have been taken by various researchers to reduce the fluoride concentration in water. Adsorbents like activated carbon, activated alumina, hydroxypatite, polymeric resins, clay, chitosan beads, limestone and low cost adsorbents were successfully tried for fluoride removal [1–10].

Alumina is an advanced material used as an adsorbent and catalyst as it possesses excellent physical and tectural properties as compared to other transitional inorganic oxides [11,12]. Alumina and alumina coated materials are used as adsorbents for fluoride and heavy metal removal [2,13–15]. Alum floc, alumina and activated alumina were extensively tried for fluoride removal. Among them, activated alumina is a promising adsorbent for the removal of fluoride in drinking water because of its high affinity for fluoride, low cost and easy regeneration. Using activated alumina defluoridation technologies have been developed and the main disadvantages are clogging of bed during scale up operations and

fouling problems caused by suspended solids due to the formation of metal hydroxides.

Due to its low cost and abundant source, alumina has become the most commonly used polymeric filler [16]. Most of the polymers are synthetic materials, their biocompatibility and biodegradability are much more limited than those of natural polymers like starch, cellulose, lignin, chitin and chitosan. Among biopolymers chitin and chitosan are recommended as suitable functional materials because these natural polymers have excellent properties such as biocompatibility, biodegradability, non-toxicity, adsorption properties, etc. [17]. Nowadays, much attention has been paid to chitosan as a potential polysaccharide resource.

Polymeric composites are a new class of materials with ultrafine phase dimensions. A number of studies have been performed on the preparation of new organic–inorganic hybrid polymeric composites which have received considerable attention in recent years due to its better handling properties [18]. Polymeric composites can be made into usable forms viz., beads, membranes, candles, etc. and environmentally sound. But the use of polymeric composites for toxic ions removal are very scanty [19–21].

The aim of this work was to synthesize alumina/chitosan (AICs) composite by dispersing the alumina particles in the chitosan polymeric matrix and to determine the ability of AICs composite to remove fluoride from aqueous solution. A comparison of the DCs of chitosan, alumina and AICs composite was made. The various influencing defluoridating parameters viz., contact time, solution pH and presence of other anions on DC of the sorbent were optimized. The experimental data was fitted with various isotherms to

* Corresponding author. Tel.: +91 451 2452371; fax: +91 451 2454466.

E-mail addresses: natrayasamy.viswanathan@rediffmail.com (N. Viswanathan), drs.meena@rediffmail.com (S. Meenakshi).

find the best-fit model for the sorption system. The suitability of AICs composite at field conditions was tested by collecting fluoride water in a nearby fluoride-endemic area.

2. Materials and methods

2.1. Materials

Chitosan (85% deacetylated) was supplied by Pelican Biotech and Chemicals Labs, Kerala (India). Alumina, glacial acetic acid, glutaraldehyde and sodium fluoride were purchased from Merck (Germany) and all other chemicals used were of analytical grade.

2.2. Synthesis of AICs composite

About 20 g of alumina (Al) was immersed in 30 mL of distilled water to make slurry. About 2 g of chitosan was dissolved in (2%, v/v) acetic acid and added to the slurry and the mixture was stirred for 30 min. About 5% of glutaraldehyde aqueous solution at a 40:1 volume ratio of chitosan was added and stirred vigorously for 5 min. Then the mixture was transferred to a refrigerator at 4 °C for 24 h to undergo cross-linking reaction and washed to neutral pH. Further, the mixture was dried in an oven at 60 °C for 3 days. The dried AICs composite is ground to powder form of uniform size and then used for fluoride sorption studies.

2.3. Sorption experiments

Defluoridation experiments were carried out by batch equilibration method in duplicate. In a typical case, 0.1 g of the sorbent was added to 50 mL of 10 mg/L initial fluoride concentration. The contents were shaken thoroughly using a thermostated shaker rotating at a speed of 200 rpm and the filtrate was analyzed for fluoride. The influence of various parameters viz., contact time, pH and presence of other anions on DC of the sorbent was investigated. For the temperature studies, the effect of different initial fluoride concentrations viz., 9, 11, 13 and 15 mg/L at 303, 313 and 323 K on sorption rate was studied by keeping the mass of sorbent as 0.1 g and volume of solution as 50 mL at neutral pH. The solution was then filtered and the residual fluoride ion concentration was measured.

2.4. Analysis

The concentration of fluoride was measured using expandable ion analyzer EA 940 and the fluoride ion selective electrode BN 9609 with the relative accuracy of ± 1 significant digit, detection limit of 0.02 mg/L and reproducibility of $\pm 2\%$ using TISAB II buffer [22]. The pH measurements were carried out with the same instrument with pH electrode. All other water quality parameters were analyzed by using standard methods [23].

2.5. Characterisation

Fourier transform infrared spectroscopy (FTIR) was carried out on JASCO-460 plus model to obtain the structural information of AICs composite. The surface morphology of the sorbent was studied with atomic force microscope (AFM) with INNOVA model, VEECO Instruments (USA) and scanning electron microscope (SEM) with HITACHI-S-3400 model. Elemental spectra of the composite were obtained using an energy dispersive X-ray analyzer (EDAX) during SEM observations which allows a qualitative detection and localization of elements in the composite. Surface area of the sorbent was obtained using Micromeritics-Tristar 3000 model.

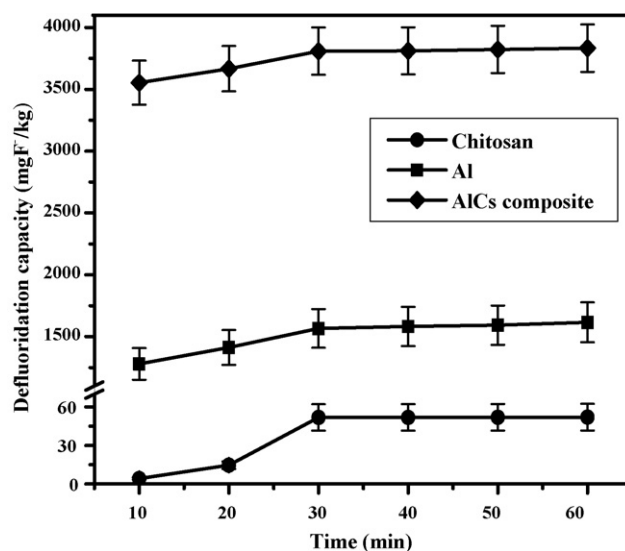


Fig. 1. Effect of contact time on DC of the sorbents at 303 K.

2.6. Statistical tools

Computations were made using Microcal Origin (Version 6.0) software. The significance of trends of data and goodness of fit was discussed using error bar plot, regression correlation coefficient (r), chi-square analysis and standard deviation (sd).

3. Results and discussion

3.1. Effect of contact time

The DCs of the chitosan, alumina and AICs composite were determined by varying the contact time in the range of 10–60 min, 0.1 g dose with 10 mg/L initial fluoride concentration in neutral pH at 303 K. As shown in Fig. 1, all the sorbents reached saturation at 30 min, therefore for further studies the contact time was fixed as 30 min. The AICs composite possesses an enhanced defluoridation capacity (DC) of 3809 mg F⁻/kg than the alumina and chitosan which have got the DCs of 1566 and 52 mg F⁻/kg. Since chitosan possesses low DC than AICs composite and Al, further studies were focused to Al and AICs composite.

3.2. Influence of solution pH

The removal of fluoride ions from aqueous solution was highly dependent on the solution pH. Hence the fluoride sorption onto the sorbents were studied at five different initial pH levels viz., 3, 5, 7, 9 and 11 by keeping 30 min as contact time, 0.1 g sorbent and 10 mg/L initial fluoride concentration at 303 K. The pH of the working solution was controlled by adding HCl/NaOH solution. Fig. 2 shows the DC of the sorbents as a function of pH. For alumina, the maximum DC was observed at acidic pH ranges and minimum DC in alkaline pH. But in case of AICs composite, though it appears that the DC of the sorbent was slightly influenced by pH of the medium, the differences are not so significant and hence it can be concluded that there is no pH dependence on DC of AICs composite which is one of the advantages of AICs composite than Al. In all the pH ranges studied, the AICs composite was found to possess higher DC than that of Al. Therefore, further studies were limited to AICs composite.

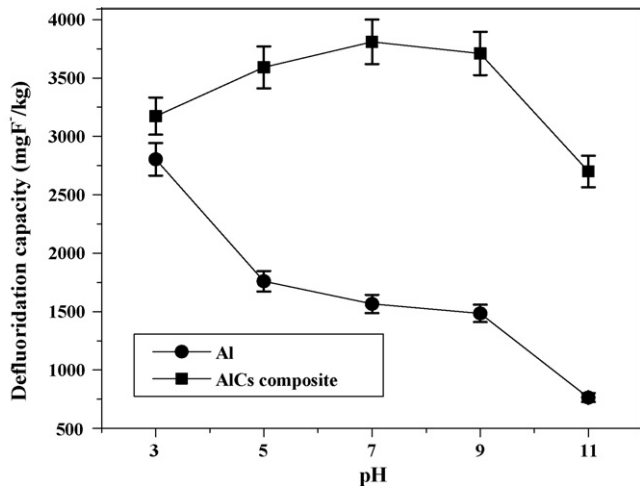


Fig. 2. Influence of pH on the DC of alumina and AlCs composite at 303 K.

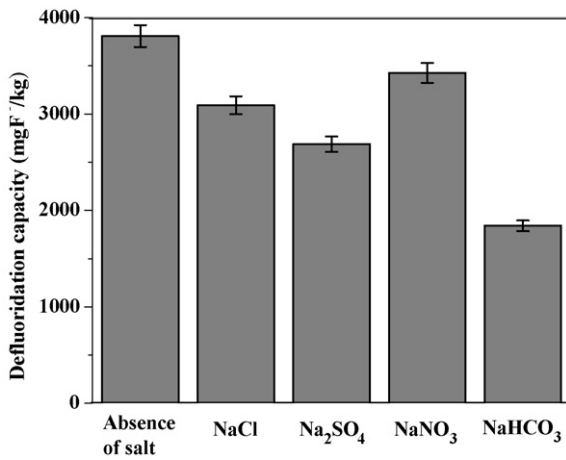


Fig. 3. Effect of co-anions on the DC of AlCs composite at 303 K.

3.3. Effect of co-anions

Fig. 3 shows the effect of DC of AlCs composite in the presence of co-anions like Cl⁻, SO₄²⁻, HCO₃⁻ and NO₃⁻ with a fixed initial

Table 1 Characteristics of alumina and AlCs composite.

| Constituents | Alumina | AlCs composite |
|--------------------------------------|---------|----------------|
| Particle size (nm) | 23.78 | 227 |
| True density (g/cm ³) | 3.69 | 0.48 |
| BET surface area (m ² /g) | 68.37 | 55.23 |

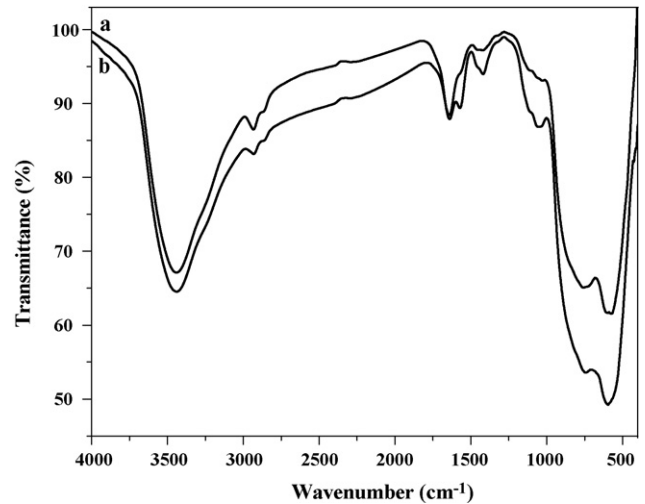


Fig. 4. FTIR spectra of (a) AlCs composite and (b) fluoride-sorbed AlCs composite.

concentration of 200 mg/L, 10 mg/L initial fluoride concentration, 30 min as contact time and 0.1 g sorbent with neutral pH at 303 K. From the graph it is evident that the overall DC of AlCs composite was slightly decreased by the presence of Cl⁻, SO₄²⁻ and NO₃⁻ ions and decreased in the presence of HCO₃⁻ ion which leads to reduction in DC. The reason could be in the presence of other anions, there may be a competition among them for the active sites on the sorbent surfaces, which is decided by the concentration, charge and size of the anions [7]. In addition to this, with an increase in bicarbonate concentration, the solution pH gets increased. Higher the pH value, lower is the number of active sites for fluoride sorption.

3.4. Characterisation of AlCs composite

The characteristics of alumina and AlCs composite are shown in Table 1. Fig. 4a and b represents the FTIR spectra of AlCs com-

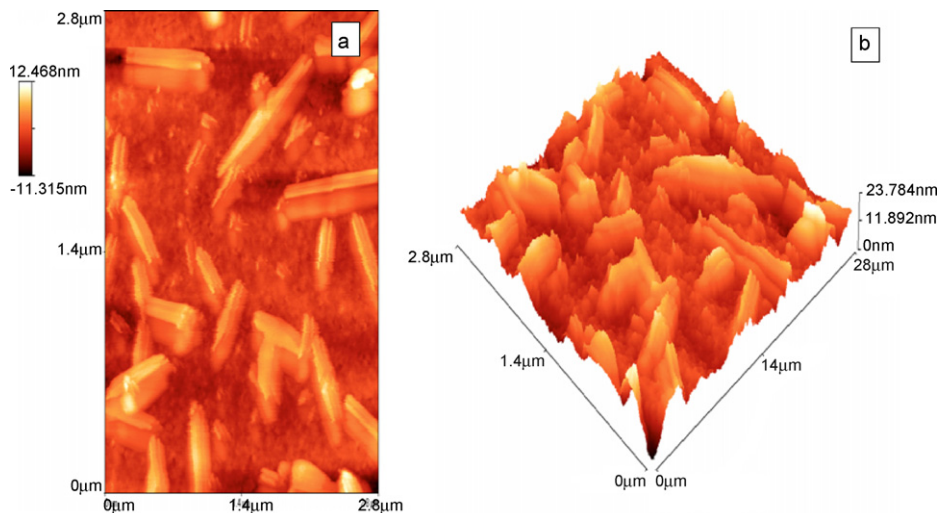


Fig. 5. AFM images of alumina (a) 2D and (b) 3D.

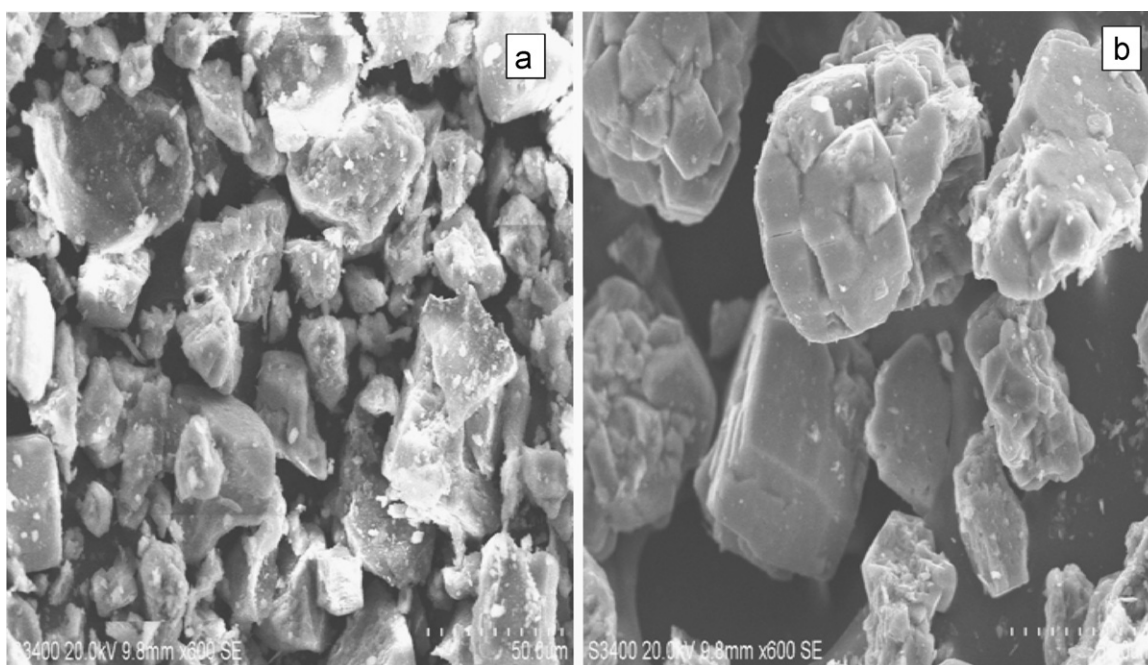


Fig. 6. SEM images at 50 μm of (a) AICs composite and (b) fluoride-sorbed AICs composite.

posite and fluoride-sorbed AICs composite. The broad band at 3440 cm^{-1} indicates the presence of $-\text{OH}$ and $-\text{NH}$ stretching vibrations. The band at 2921 cm^{-1} indicates the $-\text{CH}$ stretching vibration in $-\text{CH}$ and $-\text{CH}_2$. A band at 1639 cm^{-1} corresponds to $-\text{NH}$ bending vibration in $-\text{NH}_2$ and 1065 cm^{-1} indicates the presence of $-\text{CO}$ stretching vibration in $-\text{COH}$ [14]. The bands observed between 1000 and 500 cm^{-1} could be characteristic vibrations of aluminium oxide [24,25]. In addition the metal–oxygen stretching mode was observed at 625 cm^{-1} [25]. This figure reveals that all functional groups originally present on chitosan are intact, even after coating on alumina. After fluoride sorption, the band observed at 1370 cm^{-1} becomes very strong, sharp and shifts to higher wavenumber of 1385 cm^{-1} (cf. Fig. 4b). Parallel results are reported by various authors [25,26].

AFM (2D and 3D) images of alumina are shown in Fig. 5a and b respectively. The alumina particles possess cylindrical rod like structure with a particle size of 23.78 nm . SEM picture of AICs composite and the fluoride-sorbed AICs composite is shown in Fig. 6a and b respectively. The change in the SEM micrographs of the sorbent before and after fluoride treatment indicates the structural changes in the sorbent. This is further supported by EDAX analysis which provides the direct evidence for the sorption of fluoride ions onto AICs composite. The EDAX spectra of AICs composite confirm the presence of respective ions in the composite (cf. Fig. 7a). The fluoride sorption has occurred on AICs composite which was confirmed by the presence of fluoride and $\text{Al}+\text{F}$ peaks in the EDAX spectra of fluoride treated AICs composite (cf. Fig. 7b).

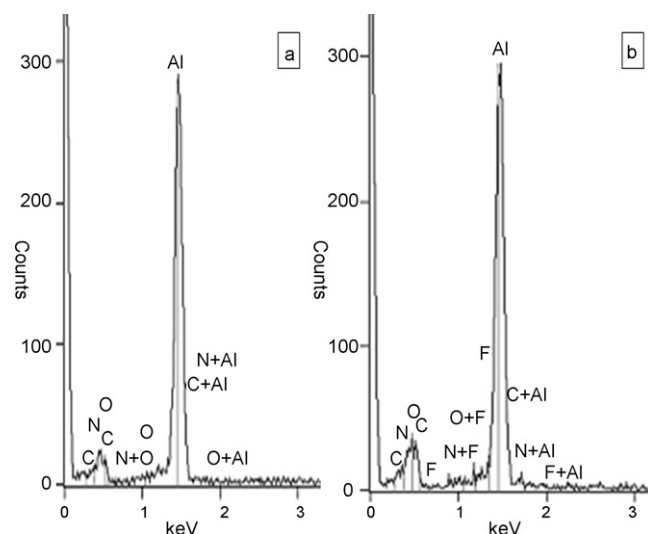


Fig. 7. EDAX spectra of (a) AICs composite and (b) fluoride treated AICs composite.

3.5. Sorption isotherms

To quantify the sorption capacity of AICs composite for fluoride sorption, two commonly used isotherms namely Freundlich and Langmuir have been adopted.

Table 2
Freundlich and Langmuir isotherms of AICs composite.

| Temp. (K) | Freundlich isotherm | | | | | Langmuir isotherm | | | | |
|-----------|---------------------|-------|------------------------------|-------|----------|-------------------|-----------|-------|-------|----------|
| | $1/n$ | n | k_F (mg/g) (L/mg) $^{1/n}$ | r | χ^2 | Q^c (mg/g) | b (L/g) | R_L | r | χ^2 |
| 303 | 0.951 | 1.052 | 1.164 | 0.999 | 2.38E-6 | 10.417 | 0.063 | 0.638 | 0.989 | 4.2E-3 |
| 313 | 0.735 | 1.361 | 1.897 | 0.999 | 8.42E-5 | 16.667 | 0.115 | 0.491 | 0.990 | 3.10E-4 |
| 323 | 0.546 | 1.832 | 2.838 | 0.998 | 3.62E-4 | 23.810 | 0.333 | 0.250 | 0.992 | 1.33E-3 |

3.5.1. Freundlich isotherm

The linear form of Freundlich [27] isotherm is represented by the equation,

$$\log q_e = \log k_F + \frac{1}{n} \log C_e \quad (1)$$

where q_e is the amount of fluoride adsorbed per unit weight of the sorbent (mg/g), C_e is the equilibrium concentration of fluoride in solution (mg/L), k_F is a measure of adsorption capacity and $1/n$ is the adsorption intensity. A linear plot of $\log q_e$ vs. $\log C_e$ indicates the applicability of Freundlich isotherm. The $1/n$ and k_F values of AICs composite are listed in Table 2. The values of $1/n$ lying between 0 and 1 and the n value lying in the range of 1–10 confirm the favorable conditions for adsorption. With the rise in temperature, the k_F values get increased which indicates that the fluoride sorption by AICs composite is an endothermic process.

3.5.2. Langmuir isotherm

Langmuir [28] isotherm model can be represented by the equation

$$\frac{C_e}{q_e} = \frac{1}{Q^\circ b} + \frac{C_e}{Q^\circ} \quad (2)$$

where Q° is the amount of adsorbate at complete monolayer coverage (mg/g), which gives the maximum sorption capacity of the sorbent and b (L/mg) is the Langmuir isotherm constant that relates to the energy of adsorption. The linear plot of C_e/q_e vs. C_e indicates the applicability of Langmuir isotherm. The values of Q° and b are listed in Table 2. The values of Q° and b increase with the rise in temperature indicating the endothermic nature of fluoride sorption.

In order to find out the feasibility of the isotherm, the essential characteristics of the Langmuir isotherm can be expressed in terms of a dimensionless constant separation factor or equilibrium parameter, R_L

$$R_L = \frac{1}{1 + bC_0} \quad (3)$$

where b is the Langmuir isotherm constant and C_0 is the initial concentration of fluoride (mg/L). The R_L values lying between 0 and 1 indicate favorable adsorption for all the temperatures studied (cf. Table 2).

3.5.3. Chi-square analysis

To identify a suitable isotherm model for the sorption of fluoride on AICs composite, this analysis has been carried out. The equivalent mathematical statement is

$$\chi^2 = \sum \frac{(q_e - q_{e,m})^2}{q_{e,m}} \quad (4)$$

where $q_{e,m}$ is equilibrium capacity obtained by calculating from the model (mg/g) and q_e is experimental data of the equilibrium capacity (mg/g). If data from the model are similar to the experimental data, χ^2 will be a small number, while if they differ, χ^2 will be a bigger number. The results of chi-square analysis are presented in Table 2. The lower χ^2 values of Freundlich isotherm than the Langmuir suggest the applicability of best-fitting model for the sorption of fluoride on AICs composite.

3.6. Thermodynamic treatment of the sorption process

Thermodynamic parameters associated with the adsorption, viz., standard free energy change (ΔG°), standard enthalpy change (ΔH°) and standard entropy change (ΔS°) were calculated as follows

Table 3

Thermodynamic parameters of AICs composite.

| Thermodynamic parameters | | AICs composite |
|--|-------|----------------|
| ΔG° (kJ mol ⁻¹) | 303 K | -8.59 |
| | 313 K | -6.41 |
| | 323 K | -4.56 |
| ΔH° (kJ mol ⁻¹) | | 69.74 |
| ΔS° (kJ mol ⁻¹ K ⁻¹) | | 0.20 |

The free energy of sorption process, considering the sorption equilibrium coefficient K_0 , is given by the equation

$$\Delta G^\circ = -RT \ln K_0 \quad (5)$$

where ΔG° is the standard free energy of sorption (kJ/mol), T is the temperature in Kelvin and R is the universal gas constant (8.314 J mol⁻¹ K⁻¹). The sorption distribution coefficient K_0 , was determined from the slope of the plot $\ln(q_e/C_e)$ against C_e at different temperatures and extrapolating to zero C_e according to the method suggested by Khan and Singh [29].

The sorption distribution coefficient may be expressed in terms of ΔH° and ΔS° as a function of temperature:

$$\ln K_0 = \frac{\Delta S^\circ}{R} - \frac{\Delta H^\circ}{RT} \quad (6)$$

where ΔH° is the standard enthalpy change (kJ/mol) and ΔS° is the standard entropy change (kJ/mol K). The values of ΔH° and ΔS° can be obtained from the slope and intercept of a plot of $\ln K_0$ against $1/T$.

The calculated values of thermodynamic parameters are shown in Table 3. The negative values of ΔG° indicate the spontaneous nature of fluoride sorption onto AICs composite. The value of ΔH° is positive indicating that the sorption process is endothermic. The positive value of ΔS° shows the increased randomness at the solid/solution interface during fluoride sorption.

3.7. Sorption kinetic models

The two main types of sorption kinetic models namely reaction-based and diffusion-based models were adopted to fit the experimental data.

3.7.1. Reaction-based models

The most commonly used pseudo-first-order and pseudo-second-order models were employed to explain the solid/liquid adsorption.

A simple pseudo-first-order kinetic model [30] is given as.

$$\log(q_e - q_t) = \log q_e - \frac{k_{ad}}{2.303} t \quad (7)$$

where q_t is the amount of fluoride on the surface of the composite at time t (mg/g) and k_{ad} is the equilibrium rate constant of the pseudo-first-order sorption (min⁻¹). The linear plots of $\log(q_e - q_t)$ against t give straight line indicate the applicability of pseudo-first-order model. The slope of the straight line plot of $\log(q_e - q_t)$ against t sorption at different temperatures viz., 303, 313 and 323 K give the value of the pseudo-first-order rate constant (k_{ad}) and r are listed in Table 4.

In addition, the pseudo-second-order model is also widely used. There are four types of linear pseudo-second-order kinetic models [31] the most popular linear form is

$$\frac{t}{q_t} = \frac{1}{h} + \frac{t}{q_e} \quad (8)$$

where $q_t = q_e^2 kt / (1 + q_e kt)$, amount of fluoride on the surface of the composite at any time, t (mg/g), k is the pseudo-second-order rate

Table 4
Kinetic models of AICs composite on fluoride removal.

| Kinetic models | Parameters | 303 K | | | | 313 K | | | | 323 K | | | |
|-------------------------|----------------------------------|--------|---------|---------|---------|--------|---------|---------|---------|--------|---------|---------|---------|
| | | 9 mg/L | 11 mg/L | 13 mg/L | 15 mg/L | 9 mg/L | 11 mg/L | 13 mg/L | 15 mg/L | 9 mg/L | 11 mg/L | 13 mg/L | 15 mg/L |
| Pseudo-first-order | k_{ad} (min^{-1}) | 0.127 | 0.117 | 0.113 | 0.090 | 0.154 | 0.120 | 0.117 | 0.136 | 0.124 | 0.127 | 0.129 | 0.115 |
| | r | 0.937 | 0.966 | 0.989 | 0.986 | 0.977 | 0.969 | 0.991 | 0.980 | 0.965 | 0.948 | 0.992 | 0.975 |
| | sd | 0.213 | 0.142 | 0.075 | 0.069 | 0.153 | 0.140 | 0.072 | 0.126 | 0.158 | 0.194 | 0.075 | 0.121 |
| Pseudo-second-order | q_e (mg/g) | 3.165 | 3.831 | 4.484 | 5.128 | 3.521 | 4.132 | 4.808 | 5.495 | 3.788 | 4.425 | 5.102 | 5.780 |
| | k (g/mg min) | 0.348 | 0.349 | 0.742 | 0.927 | 0.266 | 0.378 | 0.618 | 0.360 | 0.258 | 0.381 | 0.526 | 0.416 |
| | h (mg/g min) | 3.484 | 5.128 | 14.925 | 24.390 | 3.300 | 6.452 | 14.286 | 10.870 | 3.704 | 7.463 | 13.699 | 13.889 |
| | r | 0.999 | 0.999 | 1.00 | 1.00 | 0.999 | 0.999 | 1.00 | 0.999 | 0.999 | 0.999 | 0.999 | 0.999 |
| | sd | 0.063 | 0.040 | 0.008 | 0.010 | 0.068 | 0.038 | 0.007 | 0.016 | 0.068 | 0.037 | 0.013 | 0.017 |
| Particle diffusion | k_p (min^{-1}) | 0.126 | 0.116 | 0.112 | 0.089 | 0.155 | 0.120 | 0.119 | 0.137 | 0.127 | 0.128 | 0.130 | 0.116 |
| | r | 0.937 | 0.966 | 0.989 | 0.986 | 0.977 | 0.969 | 0.991 | 0.980 | 0.965 | 0.948 | 0.992 | 0.975 |
| | sd | 0.489 | 0.326 | 0.174 | 0.159 | 0.352 | 0.322 | 0.166 | 0.291 | 0.364 | 0.447 | 0.172 | 0.279 |
| Intraparticle diffusion | k_i (mg/g $\text{min}^{0.5}$) | 0.103 | 0.099 | 0.055 | 0.038 | 0.126 | 0.088 | 0.065 | 0.101 | 0.119 | 0.083 | 0.071 | 0.083 |
| | r | 0.954 | 0.987 | 0.965 | 0.998 | 0.974 | 0.994 | 0.974 | 0.993 | 0.989 | 0.992 | 0.985 | 0.997 |
| | sd | 0.044 | 0.022 | 0.020 | 0.003 | 0.039 | 0.012 | 0.020 | 0.016 | 0.024 | 0.014 | 0.016 | 0.009 |

constant (g/mg min), q_e is the amount fluoride ion sorbed at equilibrium (mg/g) and the initial sorption rate, $h = kq_e^2$ (mg/g min). The value of q_e (1/slope), k (slope²/intercept) and h (1/intercept) of the pseudo-second-order equation can be found out experimentally by plotting t/q_t against t . The values of q_e , k , h and r of the pseudo-second-order model were obtained from the plots of t/q_t vs. t for fluoride sorption at different temperatures viz., 303, 313 and 323 K of AICs composite are presented in Table 4. The values of q_e increase with the increase in temperature indicating the fluoride sorption increases with rise in temperature. The higher r values obtained for pseudo-second-order model than pseudo-first-order model indicate the applicability of the pseudo-second-order model.

3.7.2. Diffusion-based models

For a solid-liquid sorption process, the solute transfer is usually characterised either by particle diffusion or by intraparticle diffusion control.

A simple equation for the particle diffusion controlled sorption process [8,32] is given as follows,

$$\ln\left(1 - \frac{C_t}{C_e}\right) = -k_p t \quad (9)$$

where k_p is the particle rate constant (min^{-1}). The value of particle rate constant is obtained by the slope of the plot $\ln(1 - C_t/C_e)$ against t .

The intraparticle diffusion model used here refers to the theory proposed by Weber and Morris [33] and its equation is

$$q_t = k_i t^{1/2} \quad (10)$$

where k_i is the intraparticle rate constant (mg/g $\text{min}^{0.5}$). The slope of the plot of q_t against $t^{1/2}$ will give the value of intraparticle rate constant.

The respective straight line plots of $\ln(1 - C_t/C_e)$ vs. t and q_t vs. $t^{0.5}$ indicate the applicability of particle and intraparticle diffusion models. The k_p , k_i and r values at different temperatures viz., 303, 313 and 323 K for both particle and intraparticle diffusion models are illustrated in Table 4. The r values obtained for both particle and intraparticle diffusion models are almost comparable and suggest that the fluoride diffusion on AICs composite follows both the models.

3.7.3. The best-fit model

The assessment of the employed kinetic models for fitting the sorption data was made by standard deviation (sd). The sd values of AICs composite for all the kinetic models are shown in Table 4. Smaller sd values were observed for pseudo-second-order

and intraparticle diffusion models indicates that these two models are significant in defining the fluoride sorption process suggesting that the sorption of fluoride is onto the pores of AICs composite.

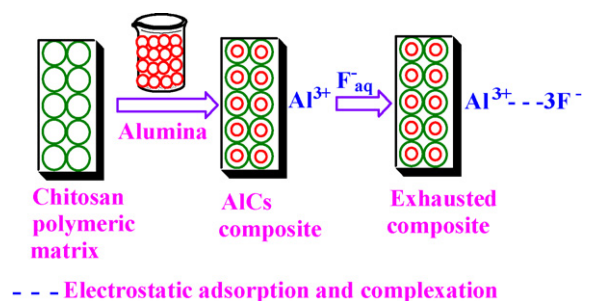
3.8. Fluoride sorption mechanism of AICs composite

The fluoride removal by AICs composite was mainly governed by electrostatic adsorption/complexation mechanism and the possible mechanism is shown in Scheme 1. The positive charge Al^{3+} at the surface of the composite attracts negatively charged fluoride ions by means of electrostatic attraction. Simultaneously the positive surface may attract fluoride by complexation too as fluoride acts as a chelating agent. The presence of Al + F peak in the EDAX spectra of fluoride treated AICs composite confirms the fluoride sorption have occurred onto AICs composite (cf. Fig. 7b). The enhancement in DC of AICs composite over Al may be due to the advantages of the combined effect of both chitosan and alumina.

A comparison of the DCs of the adsorbents reported for fluoride removal with that of AICs composite was made and is presented in Table 5. AICs composite possess an enhanced DC which confirms its selectivity toward fluoride.

3.9. Field study

AICs composite used in the present study is also tested with field sample taken from a nearby fluoride-endemic village. About 0.1 g of sorbent was added to 50 mL of fluoride water sample and the contents were shaken with constant time at room temperature. These results are presented in Table 6. There is a significant reduction in the levels of other water quality parameters in addition to fluoride. It is evident from the result that the sorbent, AICs composite can be effectively employed for removing the fluoride from water.



Scheme 1. Mechanism of fluoride sorption by AICs composite.

Table 5
A comparison of the DCs of a few reported sorbents for fluoride removal.

| Sorbents | Defluoridation capacity (mg F ⁻ /kg) | References |
|---|---|--------------------|
| AlCs composite | 3809 | Present study [34] |
| Nano-hydroxyapatite/chitin composite | 2840 | |
| Polyacrylamide Ce(IV) phosphate | 2290 | [35] |
| Polyacrylamide Zr(IV) phosphate | 2166 | [35] |
| Polyacrylamide Al(III) phosphate | 2144 | [35] |
| Activated alumina | 2136 | [2] |
| Zirconium(IV) tungstophosphate/chitosan composite | 2025 | [36] |
| Nano-hydroxyapatite/chitosan composite | 1560 | [19] |
| Nano-hydroxyapatite | 1296 | [3] |
| Protonated chitosan beads | 1664 | [37] |
| Carboxylated chitosan beads | 1385 | [7] |
| Modified kaolinite clay | 106 | [6] |
| Commercial ion exchange resin | 97 | [5] |

Table 6
Field trial results of AlCs composite.

| Water quality parameters | Treatment | |
|-------------------------------|-----------|--------|
| | Before | After |
| F ⁻ (mg/L) | 2.48 | 1.07 |
| pH | 8.52 | 8.15 |
| Cl ⁻ (mg/L) | 390.00 | 302.00 |
| Total hardness (mg/L) | 420.00 | 318.00 |
| Total dissolved solids (mg/L) | 800.00 | 637.00 |

4. Conclusions

AlCs composite possessed higher DC than alumina and chitosan. The DC of AlCs composite was not influenced by the pH of the medium and decreased in presence of bicarbonate. The sorption of fluoride on AlCs composite followed Freundlich isotherm. The nature of the reaction was spontaneous and endothermic. The fluoride removal of AlCs composite is mainly controlled by electrostatic adsorption and complexation mechanism. Field trial studies indicated that AlCs composite could be used as an effective defluorinating agent.

Acknowledgements

The corresponding author was grateful to University Grants Commission (No. F.30-56/2004(SR)), New Delhi, India for the provision of financial support to carry out this research work.

References

- [1] Y.H. Li, S. Wang, X. Zhang, J. Wei, C. Xu, Z. Luan, D. Wu, Adsorption of fluoride from water by aligned carbon nanotubes, *Mater. Res. Bull.* 38 (2003) 469–476.
- [2] G. Karthikeyan, A. Shanmuga Sundarraj, S. Meenakshi, K.P. Elango, Adsorption dynamics and the effect of temperature of fluoride at alumina–solution interface, *J. Indian Chem. Soc.* 81 (2004) 461–466.

- [3] C. Sairam Sundaram, N. Viswanathan, S. Meenakshi, Defluoridation chemistry of synthetic hydroxyapatite at nano scale: equilibrium and kinetic studies, *J. Hazard. Mater.* 155 (2008) 206–215.
- [4] Y. Ku, H.M. Chiou, W. Wang, The removal of fluoride ion from aqueous solution by a cation synthetic resin, *Sep. Sci. Technol.* 37 (2002) 89–103.
- [5] S. Meenakshi, N. Viswanathan, Identification of selective ion exchange resin for fluoride sorption, *J. Colloid Interface Sci.* 308 (2007) 438–450.
- [6] S. Meenakshi, C. Sairam Sundaram, R. Sukumar, Enhanced fluoride sorption by mechanochemically activated kaolinites, *J. Hazard. Mater.* 153 (2008) 164–172.
- [7] N. Viswanathan, C. Sairam Sundaram, S. Meenakshi, Sorption behaviour of fluoride on carboxylated cross-linked chitosan beads, *Colloid Surf. B* 68 (2009) 48–54.
- [8] N. Viswanathan, S. Meenakshi, Enhanced fluoride sorption using La(III) incorporated carboxylated chitosan beads, *J. Colloid Interface Sci.* 322 (2008) 375–383.
- [9] E.J. Reardon, Y. Wang, A limestone reactor for fluoride removal from wastewaters, *Environ. Sci. Technol.* 34 (2000) 3247–3253.
- [10] X. Fan, D.J. Parker, M.D. Smith, Adsorption kinetics of fluoride on low cost materials, *Water Res.* 37 (2003) 4929–4937.
- [11] Y. Kim, C. Kim, I. Choi, S. Rengaraj, J. Yi, Arsenic removal using mesoporous alumina prepared via a templating method, *Environ. Sci. Technol.* 38 (2004) 924–931.
- [12] Z. Zhang, T.J. Pinnavaia, Mesostructured γ -Al₂O₃ with a lathlike framework morphology, *J. Am. Chem. Soc.* 124 (2002) 12294–12301.
- [13] M. Revathi, B. Kavitha, T. Vasudevan, Removal of nickel ions from industrial plating effluents using activated alumina as adsorbent, *J. Environ. Sci. Eng.* 47 (2005) 1–6.
- [14] V.M. Boddu, K. Abburi, J.L. Talbott, E.D. Smith, R. Haasch, Removal of arsenic (III) and arsenic (V) from aqueous medium using chitosan-coated biosorbent, *Water Res.* 42 (2008) 633–642.
- [15] C.S. Boruff, A.M. Buswell, W.V. Upton, Adsorption of fluoride from salts by alum floc, *Ind. Eng. Chem.* 29 (1937) 1154.
- [16] B.J. Ash, D.F. Rogers, C.J. Weigand, L.S. Schadler, R.W. Siegel, B.C. Benicewicz, T. Apple, Mechanical properties of Al₂O₃/polymethylmethacrylate nanocomposites, *Polym. Composite* 23 (2002) 1014–1025.
- [17] R.A.A. Muzzarelli, *Natural Chelating Polymers: Alginic Acid, Chitin and Chitosan*, Pergamon Press, New York, 1973.
- [18] W.J.E.M. Habraken, J.G.C. Wolke, J.A. Jansen, Ceramic composites as matrices and scaffolds for drug delivery in tissue engineering, *Adv. Drug Deliv. Rev.* 59 (2007) 234–248.
- [19] C. Sairam Sundaram, N. Viswanathan, S. Meenakshi, Uptake of fluoride by nano-hydroxyapatite/chitosan, a bioinorganic composite, *Bioresour. Technol.* 99 (2008) 8226–8230.
- [20] C. Sairam Sundaram, N. Viswanathan, S. Meenakshi, Defluoridation of water using magnesite/chitosan composite, *J. Hazard. Mater.* 163 (2009) 618–624.
- [21] X. Liu, Q. Hu, Z. Fang, X. Zhang, B. Zhang, Magnetic chitosan nanocomposites: a useful recyclable tool for heavy metal ion removal, *Langmuir* 25 (2009) 3–8.
- [22] Fluoride Electrode Instruction Manual, Orion Research, USA, 2005.
- [23] APHA, Standard Methods for the Examination of Water and Waste Water, American Public Health Association, Washington, DC, 2005.
- [24] D.P. Das, J. Das, K. Parida, Physicochemical characterization and adsorption behaviour of calcined Zn/Al hydrotalcite-like compound towards removal of fluoride from aqueous solution, *J. Colloid Interface Sci.* 261 (2003) 213–220.
- [25] A. Legrouri, M. Badreddine, A. Barroug, A.D. Roy, J.P. Besse, Influence of pH on the synthesis of the Zn–Al–nitrate layered double hydroxide and the exchange of nitrate by phosphate ions, *J. Mater. Sci. Lett.* 18 (1999) 1077–1079.
- [26] F. Cavani, F. Trifiro, A. Vaccari, Hydrotalcite-type anionic clays: preparation, properties and applications, *Catal. Today* 11 (1991) 173–301.
- [27] H.M.F. Freundlich, Über die adsorption in lösungen, *Z. Phys. Chem.* 57A (1906) 385–470.
- [28] I. Langmuir, The constitution and fundamental properties of solids and liquids, *J. Am. Chem. Soc.* 38 (1916) 2221–2295.
- [29] A.A. Khan, R.P. Singh, Adsorption thermodynamics of carbofuran on Sn (IV) arsenosilicate in H⁺, Na⁺ and Ca²⁺ forms, *Colloids Surf.* 24 (1987) 33–42.
- [30] S. Lagergren, Zur theorie der sogenannten adsorption gelöster stoffe, *K. Sven. Vetenskapsakad. Handl.* 24 (1898) 1–39.
- [31] Y.S. Ho, Second order kinetic model for the sorption of cadmium on to tree fern: a comparison of linear and non linear methods, *Water Res.* 40 (2006) 119–125.
- [32] M. Chanda, K.F. O'Driscoll, G.L. Rempel, Sorption of phenolics onto cross-linked poly (4-vinyl pyridine), *React. Polym.* 1 (1983) 281–293.
- [33] W.J. Weber, J.C. Morris, Equilibria and capacities for adsorption on carbon, *J. Sanitary Eng. Div.* 90 (1964) 79–91.
- [34] C. Sairam Sundaram, N. Viswanathan, S. Meenakshi, Fluoride sorption by nano-hydroxyapatite/chitin composite, *J. Hazard. Mater.* 172 (2009) 147–151.
- [35] C. Sairam Sundaram, S. Meenakshi, Fluoride sorption using organic–inorganic hybrid type ion exchangers, *J. Colloid Interface Sci.* 333 (2009) 58–62.
- [36] N. Viswanathan, S. Meenakshi, Development of chitosan supported zirconium(IV) tungstophosphate composite for fluoride removal, *J. Hazard. Mater.* 176 (2010) 459–465.
- [37] N. Viswanathan, C. Sairam Sundaram, S. Meenakshi, Removal of fluoride from aqueous solution using protonated chitosan beads, *J. Hazard. Mater.* 161 (2009) 423–430.